Sensors & Transducers, Vol. 272, Issue 1, April 2026, pp. 36-49

www.sensorsportal.com

Sensors & Transducers

Published by IFSA Publishing, S. L., 2026
http://www.sensorsportal.com

Joint Rotor Speed Scheduling and Trajectory Optimization for Energy-Efficient Electric UAV Rotorcraft Missions

*** Emeka CHIJIOKE and Marcin ŻUGAJ**
Warsaw University of Technology, pl. Politechniki 1, 00-661 Warsaw, Poland
Tel.: +48 222347220
* E-mail: emeka.chijioke.dokt@pw.edu.pl

Received: 19 Jan. 2026 /Revised:13 April 2026 /Accepted: 20 April 2026 /Published:28 April 2026

Abstract: Electric unmanned rotorcraft are increasingly considered for aerial mobility applications, but their performance is limited by onboard energy storage, making energy efficiency a critical design consideration. This study investigates the effects of rotor speed scheduling and trajectory optimization on total mission energy consumption for a hover–ascent–cruise–descent profile. A mission-based energy model is developed to estimate rotor power and cumulative energy across all flight phases. A sequential optimization framework is adopted, in which rotor speed optimization is first performed to determine a phase-dependent rotor speed schedule, followed by trajectory optimization conducted under a fixed rotor speed profile obtained from the preceding stage, with only trajectory parameters allowed to vary. A joint optimization is then evaluated to assess the integrated effect of both strategies. Results show that rotor speed optimization reduces energy by 21.85 %, while trajectory optimization achieves a larger reduction of 24.99 %. The joint optimization yields the lowest energy consumption, with a total reduction of 25.01 %, providing only a marginal improvement over trajectory optimization. These findings indicate that trajectory design is the dominant contributor to energy savings, while rotor speed scheduling offers complementary benefits for improving rotorcraft endurance.

Keywords: Rotor speed scheduling, Trajectory optimization, Energy consumption, Energy-efficient flight, Electric rotorcraft, UAV, Mission energy optimization.

1. Introduction

This article is an extended version of the conference paper presented in [1], where a preliminary version of this work was introduced, including the staged optimization framework and initial simulation results. The present work includes additional analysis, expanded methodology, extended results, and deeper discussion of the coupled effects between rotor speed scheduling and trajectory optimization.

The methodology is further refined through the formulation of a clearly defined sequential optimization framework, in which rotor speed optimization is performed prior to trajectory optimization using a fixed rotor speed schedule, with only trajectory parameters allowed to vary. In addition, the work includes expanded parametric analyses, improved figure presentation, and a more comprehensive comparison of energy consumption across rotor speed, trajectory, and joint optimization strategies. The results are also critically reassessed to account for numerical sensitivity and modeling limitations, providing a more rigorous evaluation of the relative contributions of each optimization approach.

Unmanned aerial vehicle (UAV) electric rotorcraft are gaining increasing attention in both civil and military aerospace applications due to their potential for reduced emissions, lower operating costs, and quieter operation compared with conventional fuel

powered platforms. These advantages have made electric vertical takeoff and landing (eVTOL) vehicles and unmanned rotorcraft particularly attractive for emerging applications such as urban air mobility, infrastructure inspection, environmental monitoring, and short-range transportation [2, 3]. Despite these benefits, the operational capability of electric rotorcraft remains strongly constrained by the relatively low energy density of current battery technologies. As a result, improving mission energy efficiency has become a critical research challenge in the design and operation of electrically powered aerial vehicles [4].

The energy consumption of a rotorcraft mission is determined by a combination of aerodynamic, propulsion, and flight mechanics factors that vary across different flight phases. Hover and climb segments typically require high induced power, while cruise flight is dominated by parasite drag and forward flight aerodynamic effects [5, 6]. Consequently, the total mission energy demand depends not only on the rotor performance characteristics but also on the trajectory followed during the mission. Operational parameters such as rotor rotational speed, flight velocity, and climb or descent rates can significantly influence the power required to sustain flight. Optimizing these parameters therefore offers a practical pathway for improving rotorcraft endurance without major hardware modifications.

One approach that has received considerable attention is rotor speed scheduling. Variable rotor speed operation allows the rotor to operate closer to its optimal aerodynamic efficiency under varying flight conditions. Higher rotor speeds may be beneficial in hover or low speed flight, while lower rotor speeds during cruise can reduce profile power and mechanical losses. Previous studies have demonstrated that adaptive rotor speed control can reduce power consumption and improve endurance in both conventional helicopters and electric rotorcraft [7-9]. However, rotor speed optimization alone does not account for the influence of the mission trajectory on aerodynamic loading and overall energy demand.

Another important strategy for improving energy efficiency involves trajectory optimization. By adjusting parameters such as cruise velocity, climb rate, and descent rate, rotorcraft can operate closer to aerodynamic conditions that minimize power requirements. Efficient trajectory planning can reduce unnecessary altitude changes, avoid unfavorable environmental conditions, and improve overall mission energy performance. Previous work has shown that routing strategies that consider wind conditions and energy-efficient path planning can significantly reduce the energy required to complete UAV missions [10].

Although rotor speed scheduling and trajectory optimization have each been studied independently [11-13], the interaction between these two control strategies has received comparatively less attention. Rotor speed directly influences rotor aerodynamic efficiency, while trajectory parameters determine the aerodynamic loading experienced during flight. Because these variables are inherently coupled, optimizing them independently may not fully exploit the potential for mission energy reduction. In particular, it remains unclear to what extent rotor speed variation continues to provide benefits once the trajectory has already been optimized.

The objective of the present study is therefore to develop a mission-based energy model for electric rotorcraft covering hover, ascent, cruise, and descent phases. Using this model, three optimization strategies are implemented and compared, namely rotor speed optimization with a baseline trajectory, trajectory optimization using the rotor speed schedule obtained from the previous stage, and joint optimization in which both rotor speed and trajectory parameters are adjusted simultaneously. The results are analyzed to quantify the relative contribution of each strategy to mission energy reduction and to identify the dominant factors influencing rotorcraft energy efficiency.

2. Literature Review

Research on rotorcraft energy efficiency has primarily focused on three key areas, namely aerodynamic modeling of rotor performance, rotor speed control strategies, and trajectory optimization for UAV missions. These aspects are closely interconnected, as energy consumption depends not only on rotor aerodynamics but also on how the vehicle is controlled and operated along its flight path. The following sections review the main developments in each of these areas.

2.1. Aerodynamic Power Modeling

Early investigations into rotorcraft power consumption focused on the development of analytical models for estimating rotor aerodynamic performance. Momentum theory and blade element methods have been widely used to estimate induced, profile, and parasite power contributions during different flight conditions [5, 6]. These models form the foundation for predicting rotorcraft energy consumption during hover and forward flight. Subsequent studies incorporated additional aerodynamic effects such as rotor inflow dynamics, blade drag characteristics, and forward flight performance, enabling more accurate estimation of rotorcraft power requirements across complete mission profiles.

2.2. Variable Rotor Speed Operation

Several studies have investigated the benefits of variable rotor speed operation. Traditional helicopters typically operate at nearly constant rotor speeds to simplify control and maintain stable aerodynamic conditions. However, advances in electric propulsion systems and motor control technologies have enabled

more flexible rotor speed management. Adjusting rotor speed according to flight conditions can reduce power consumption by allowing the rotor to operate closer to its optimal aerodynamic efficiency [7-9]. In [14], a trajectory tracking control method for a helicopter UAV based on a kinematic model and feedback linearization was proposed. The controller adjusts forward velocity to improve tracking performance while reducing energy expenditure. Such studies demonstrate that rotor speed management can play an important role in improving UAV energy efficiency.

2.3. Trajectory Optimization

Another important area of research involves trajectory optimization for minimizing UAV energy consumption. Trajectory planning methods aim to reduce unnecessary altitude variations, minimize aerodynamic drag, and exploit favorable environmental conditions. Although trajectory optimization has been extensively studied for fixed wing UAVs [15-17], these methods cannot be directly applied to rotorcraft systems because rotor power requirements depend strongly on rotor aerodynamic loading and induced velocity effects. For rotorcraft UAVs, [18] proposed a control framework based on Model Predictive Control (MPC) that operates in real-time, allowing UAVs to adapt their trajectories dynamically while minimizing altitude variations and travel distance.

More recent studies have incorporated environmental wind effects into trajectory planning. In [10], realistic urban wind fields were generated using the Parallelized Large-Eddy Simulation Model (PALM) and integrated into an enhanced A-star search algorithm for UAV trajectory optimization. The results demonstrated that exploiting wind information during path planning can significantly reduce energy consumption compared with conventional shortest path approaches. Similarly, [19] proposed a planning framework based on an energy map that evaluates energy requirements of UAV components within a three-dimensional (3D) environment and uses heuristic graph search algorithms to determine energy-efficient trajectories. In [20], energy-efficient trajectory planning for a quadrotor UAV was formulated as an optimal control problem using a power loss model that accounts for rotor speed and acceleration.

2.4. Research Gap

Despite these advances, most existing studies optimize either rotor speed scheduling or trajectory design independently. However, because rotor speed influences aerodynamic efficiency while trajectory parameters determine aerodynamic loading during flight, these two mechanisms are inherently coupled. Understanding their interaction is therefore essential for identifying effective strategies to reduce rotorcraft mission energy consumption. To address this limitation, the present study evaluates rotor speed scheduling, trajectory optimization, and their joint implementation within a unified mission-based energy framework.

3. Methodology

3.1. Simulation and Optimization Framework

The methodology presented in this work builds upon the framework introduced in the conference paper [1], while extending it through a more comprehensive optimization formulation and a detailed analysis of the interaction between rotor speed scheduling and trajectory design.

The simulation workflow integrates MATLAB/Simulink for supervisory scheduling and command shaping with FLIGHTLAB's nonlinear six degrees of freedom (6DoF) rotorcraft model to capture high fidelity flight dynamics and aerodynamics. The combined environment enables consistent evaluation of rotorcraft performance under varying control strategies.

Mission simulations generate time-series outputs including altitude, airspeed, vertical speed, rotor speed, power consumption, and cumulative energy. These outputs are interpolated to a common time base to allow direct comparison across different optimization scenarios. An overview of the methodology workflow is shown in Fig. 1.

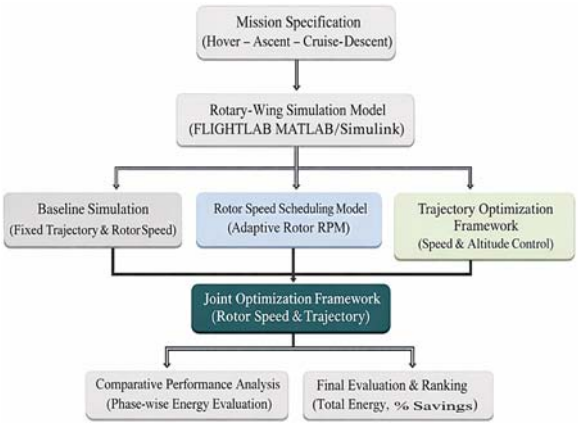

Fig. 1. Optimization framework for rotor speed and trajectory design (adapted from [1]).

3.2. Mission-Based Energy Modeling

A mission-based energy modeling approach is used to evaluate rotorcraft power consumption across different flight phases, including hover, ascent, cruise, and descent. The model captures the variation in aerodynamic and propulsion requirements across

these phases and enables estimation of cumulative electrical energy consumption over the mission duration.

Total mission energy is computed as the time integral of electrical power:

$$E(t_{end}) = \frac{1}{3600}\int_0^{t_{end}} P_e(t)\,dt, \quad (1)$$

where $P_e(t)$ is the electrical power obtained from a two-dimensional (2D) lookup table parameterized by rotor speed and shaft torque and includes aggregated drivetrain losses [21]. The model accounts for variations in power demand resulting from changes in rotor speed, flight velocity, and trajectory profile.

3.3. Rotor Speed Scheduling Model

Rotor speed scheduling is implemented using phase-dependent setpoints corresponding to hover, ascent, cruise, and descent. The rotor speed profile is parameterized as:

$$X_\Omega = [\Omega_{hover}\ \Omega_{ascent}\ \Omega_{cruise}\ \Omega_{descent}]^T \quad (2)$$

The rotor speed commands are subject to actuator and dynamic constraints. A maximum slew rate constraint:

$$\left|\frac{d\Omega}{dt}\right| \le 10\text{RPM/s} \quad (3)$$

is imposed, and a first order filter:

$$G(s) = \frac{1}{\tau s + 1} \quad (4)$$

is applied to represent rotor dynamic response. This formulation enables evaluation of how phase-dependent rotor speed adjustments influence power consumption and mission energy.

3.4. Trajectory Optimization Formulation

The mission trajectory is parameterized using key flight variables, including phase-dependent true airspeeds (TAS) and cruise altitude:

$$X_V = [V_{ascent}, V_{cruise}, V_{descent}, h_{cruise}]^T, \quad (5)$$

Trajectory commands are constrained to ensure physically realistic transitions. Rate limits are imposed on velocity and altitude profiles:

$$\left|\frac{dV}{dt}\right| \le 12 ft/s^2\ (3.7\ m/s^2), \quad (6)$$

$$\left|\frac{dh}{dt}\right| \le 5 ft/s\ (1.5\ m/s) \quad (7)$$

These constraints ensure smooth transitions between flight phases and maintain stable tracking performance within the nonlinear simulation environment.

3.5. Joint Optimization Framework

To capture the interaction between propulsion control and flight trajectory, a joint optimization framework is developed in which rotor speed scheduling and trajectory parameters are optimized simultaneously. The combined decision vector is defined as:

$$X = \begin{bmatrix} X_\Omega \\ X_V \end{bmatrix} \quad (8)$$

This formulation enables exploration of tradeoffs between aerodynamic loading and propulsion efficiency. For example, adjustments in climb rate or cruise altitude may allow lower rotor speed operation, resulting in reduced overall energy consumption.

3.6. Optimization Problem Formulation

The optimization problem is formulated as a constrained mission-based parametric search using the nonlinear rotorcraft simulation model.

The objective is to minimize total mission energy consumption:

$$\min_X J(X) = E(t_{end}), \quad (9)$$

subject to: rotor speed constraints, trajectory rate limits, flight dynamics feasibility, mission completion requirements.

The mission is divided into four phases with fixed durations: hover ($t_{hover} = 40$ s), ascent ($t_{ascent} = 30$s), cruise ($t_{cruise} = 70$ s), and descent, completing the mission at $t = 200$s.

Three optimization strategies are evaluated:

1. Rotor speed optimization with a fixed baseline trajectory, used to determine the optimal phase-dependent rotor speed schedule;
2. Trajectory optimization using the best optimal rotor speed schedule obtained from the previous stage and held constant for all cases;
3. Joint optimization of rotor speed and trajectory, performed to assess the integrated effect of both variables.

Candidate solutions are evaluated based on cumulative energy consumption, and only physically feasible trajectories with stable tracking behavior are accepted.

In contrast to the preliminary study presented in [1], the current work extends the analysis by incorporating a joint optimization framework and providing a systematic comparison of different optimization strategies. These extensions enable a

more comprehensive evaluation of the factors influencing the UAV rotorcraft mission energy efficiency.

3.7. Performance Metrics and Simulation Assumptions

Performance comparisons are conducted using both total cumulative energy consumption and flight phase energy distribution across hover, ascent, cruise, and descent segments. This allows assessment of how different optimization strategies redistribute energy demand throughout the mission profile, enabling identification of the dominant contributors to energy consumption.

To isolate the effects of rotor speed scheduling and trajectory optimization, all simulations are conducted under consistent environmental conditions. Standard atmospheric properties are assumed, with no wind or gust disturbances. This ensures that differences in energy consumption are attributable solely to variations in control inputs and trajectory parameters.

The UAV, propulsion and simulation parameters used in this study are summarized in Table 1, while the baseline mission profile is defined in Table 2. These parameters are consistent with those used in the preliminary study [1], with minor refinements introduced to support the extended analysis presented in this work.

Table 1. Rotorcraft and simulation parameters.

Parameter	Symbol	Value / Relation / Formula	Unit / Description
UAV mass	m	7.23	kg
Diameter of main rotor	D_m	1.78	m
Main rotor blade count	N_m	2	Number of blades (dimensionless)
Tail rotor diameter	D_t	0.158	m
Tail rotor blade count	N_t	2	Number of blades (dimensionless)
Baseline RPM	n_{base}	1000	RPM
Variable rotor speed range	n	850–1000	RPM
Rotor response dynamics	-	$G(s) = \frac{1}{\tau s+1}$ (with rate limiting)	First order rotor speed dynamics
Electrical power map	P_e	2D LUT: P_e (Q, n)	W (electrical input power from powertrain; function of torque and speed)
Torque calculation	Q	From rotor model	N m (main roto shaft torque)
Flight dynamics model	-	Nonlinear 6DOF rigid body model	Implemented in FLIGHTLAB
Trim methodology	-	Phase-wise steady state trim	Flight phases: hover, climb, cruise, descent
Energy model	E	$E(t_{end}) = \frac{1}{3600}\int_0^{t_{end}} P_e(t)\,dt$	Wh (time integration of electrical power P_e in W)
Atmospheric model	-	Standard atmosphere (ISA)	Assumes sea-level conditions, no environmental deviations
Wind / turbulence	-	Not considered	No wind or turbulence effects included

Table 2. Baseline mission profile parameters.

Phase	Start Time t_z (s)	Duration Δt_z (s)	Velocity V_z (ft/s [m/s])	Altitude H_z (ft [m])	Altitude Command
Hover	0	40	0	34	Constant
Ascent	40	30	60	80	Constant
Cruise	70	70	60	80	Climb rate, ±2 ft/s
Descent	140	60	55	34	Target altitude 34 ft

4. Result and Discussion

4.1. Baseline Mission Energy Characteristics

The baseline mission represents the reference operating condition against which the effectiveness of the optimization strategies is evaluated. In this configuration, the rotorcraft operates at a constant rotor speed of 1000 RPM throughout the mission while following a fixed trajectory consisting of hover, ascent, cruise, and descent phases. The resulting total mission energy consumption for the baseline case is 36.06 Wh, which represents the highest energy demand among all evaluated configurations.

Fig. 2 illustrates the baseline mission trajectory, including altitude, forward airspeed, and vertical speed, with vertical markers indicating transitions between flight phases. The rotorcraft maintains a steady hover at 34 ft (10.4 m), followed by a gradual climb to the cruise altitude of approximately 80 ft (24.4 m). This altitude is sustained during the cruise segment before a controlled descent returns the UAV to the initial hover level.

The airspeed profile reflects the prescribed mission schedule shown in Table 2, increasing from zero in hover to the cruise value of approximately 60 ft/s (18.3 m/s), and then reducing slightly during descent at 55 ft/s (16.8 m/s). The vertical speed history further confirms the phase behavior, with positive climb rates during ascent, near zero values in steady segments, and negative rates during descent, indicating smooth and continuous transitions.

Overall, the time histories demonstrate consistent tracking of the commanded flight profile, with no abrupt transients or instability. This validates the baseline trajectory as a reliable reference case for subsequent power and energy analysis.

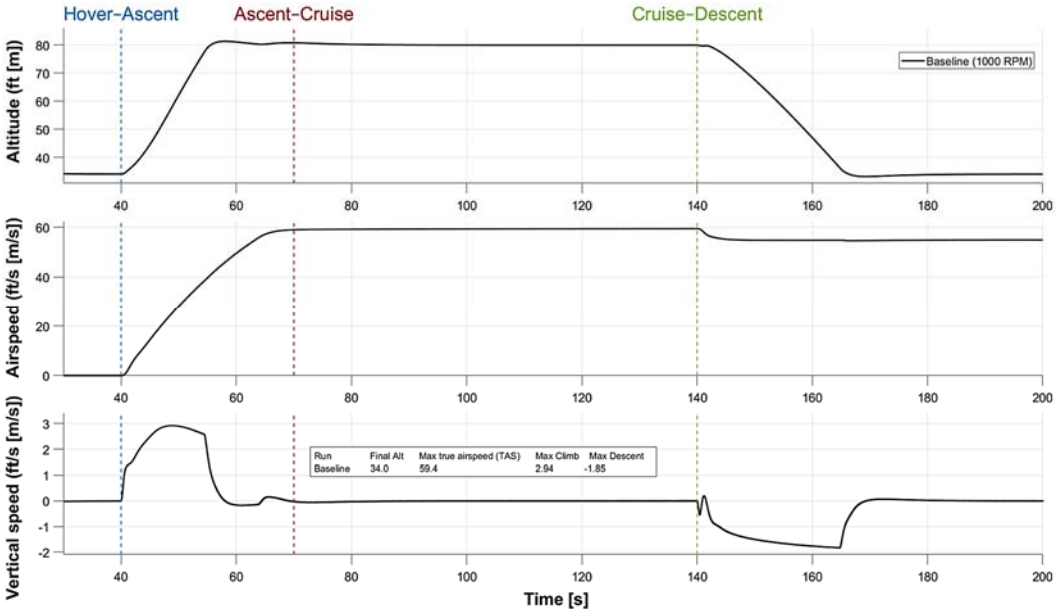

Fig. 2. Baseline mission flight profile showing altitude, forward airspeed, and vertical speed with indicated phase transitions between hover, ascent, cruise, and descent.

The baseline mission energy characteristics are illustrated using both time resolved and phase averaged representations. A constant rotor speed of 1000 RPM is used as a reference for evaluating optimization strategies.

Fig. 3 shows the time resolved main rotor (MR) power profile for the baseline mission. The hover phase exhibits the highest steady power demand approximately 591 W, dominated by induced power required to sustain lift. At the transition to ascent at 40s, a transient peak of approximately 635 W is observed due to the increased thrust required for climb. As forward speed develops, the power decreases progressively, reflecting improved aerodynamic efficiency associated with translational lift.

During cruise, the power stabilizes near 455 W, indicating steady aerodynamic conditions with reduced induced power and balanced drag contributions. At the onset of descent at 140 s, a sharp reduction in power occurs, followed by a brief transient dip, as gravitational effects reduce the required rotor thrust. The subsequent stabilization reflects controlled descent under lower power demand. These results highlight that hover and ascent phases dominate instantaneous power requirements.

The cumulative electrical energy consumption over the baseline mission is shown in Fig. 4, showing a monotonic increase over time that reflects the continuous power demand of the propulsion system across all flight phases. The slope of the curve varies slightly between segments, indicating changes in power demand associated with different operating conditions.

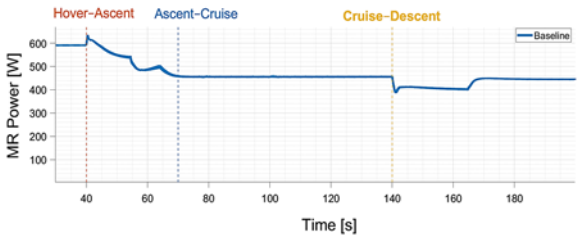

Fig. 3. Baseline main rotor power profile over the mission timeline. Phase transitions are indicated, highlighting transient responses associated with changes in flight conditions.

During hover and ascent, the energy accumulation rate is relatively higher due to increased thrust requirements. A more gradual and nearly linear trend is observed during cruise, consistent with steady operating conditions. In the descent phase, the rate of increase remains moderate, reflecting reduced power

demand compared to earlier phases while still accounting for controlled flight.

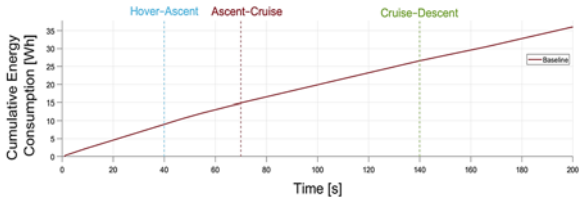

Fig. 4. Cumulative electrical energy consumption for the baseline mission.

Fig. 5 provides a phase averaged view of power demand and cumulative energy consumption for the baseline case. The blue bars represent the average power in each phase, obtained by averaging the time-resolved MR power over the corresponding phase durations. Consistent with Fig. 2, hover exhibits the highest average power, approximately 611 W, followed by ascent, 527 W, while cruise and descent phases show lower values of approximately 456 W and 429 W, respectively. The reduction in average power across phases reflects the increasing contribution of translational aerodynamic effects and reduced thrust requirements.

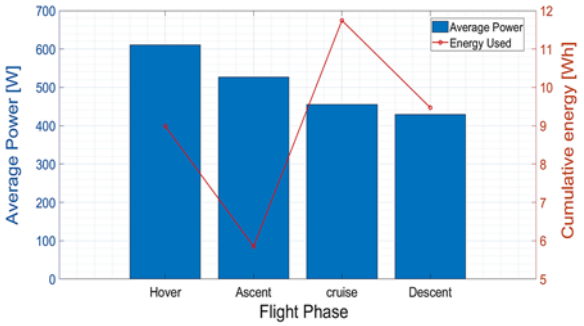

Fig. 5. Flight phase average power and cumulative energy consumption for the baseline mission profile.

The red curve represents cumulative energy consumption per phase, which depends on both power level and phase duration. Although cruise does not exhibit the highest average power, it contributes the largest energy consumption 11.7 Wh because it occupies the longest duration in the mission. In contrast, ascent consumes less energy, approximately 5.9 Wh despite moderate power demand because of its shorter duration.

These results demonstrate that hover dominates instantaneous power demand, whereas cruise dominates total energy consumption due to mission duration. Consequently, reducing cruise power or shortening cruise duration offers the greatest potential for minimizing overall mission energy.

These baseline characteristics provide a reference for evaluating how rotor speed scheduling and trajectory optimization modify both instantaneous power demand and cumulative energy consumption.

4.2. Effect of Rotor Speed Scheduling

This section evaluates the impact of rotor speed scheduling on mission energy consumption while maintaining the baseline trajectory. The rotor speed is adjusted across flight phases to improve aerodynamic efficiency and reduce power demand.

The impact of rotor speed scheduling on propulsion performance is first examined through the rotor speed time histories, as shown in Fig. 6. In the baseline configuration, the rotor speed is maintained constant at 1000 RPM throughout the mission. In contrast, the optimized schedule applies phase-dependent rotor speeds, with higher values during hover and ascent and reduced values during cruise and descent.

The optimized rotor speed decreases from approximately 925 RPM in hover to 870 RPM during cruise, reflecting a tradeoff between thrust requirements and aerodynamic efficiency. Lower rotor speeds in forward flight reduce profile power losses, while maintaining sufficient lift.

These results demonstrate that rotor speed scheduling enables adaptation of rotor operating conditions to changing aerodynamic requirements across flight phases, forming the basis for the observed reductions in power consumption and total mission energy.

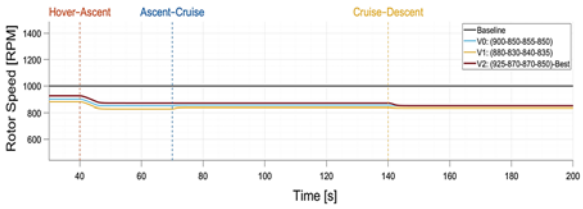

Fig. 6. Rotor speed profiles for baseline and optimized cases showing reduced rotor speed across mission phases.

The resulting changes in power demand are illustrated in Fig. 7, which compares the main rotor power profiles for the baseline and optimized cases. The optimized cases exhibit a consistent reduction in power demand across all mission phases relative to the constant speed baseline.

The most significant reduction occurs during the cruise phase, where power decreases from approximately 460 W to about 350 W. This reduction is primarily attributed to lower rotor speed, which reduces profile power losses under forward flight conditions. Due to the extended duration of cruise, this sustained reduction contributes significantly to the overall energy savings.

During hover and ascent, power reductions are also observed, although the relative improvement is moderated by the dominance of induced power, which

limits the extent of achievable savings. Nevertheless, reduced rotor speed still leads to lower overall power demand while maintaining required thrust.

In the descent phase, power demand decreases further due to both reduced thrust requirements and lower rotor speed. The optimized cases maintain consistently lower power levels while preserving smooth transitions between flight phases.

These results demonstrate that rotor speed scheduling effectively reduces power consumption, particularly in phases where profile power dominates, thereby contributing to the observed reduction in total mission energy.

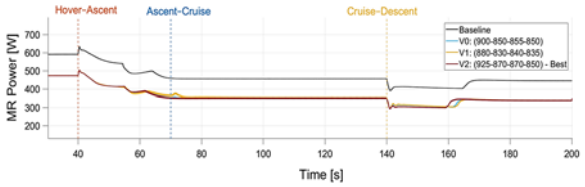

Fig. 7. Main rotor power comparison between the baseline and optimized cases showing lower power across mission phases.

The cumulative effect of these reductions is presented in Fig. 8, which shows the total energy consumption over time. All optimized cases exhibit a consistently lower rate of energy accumulation compared to the baseline, indicating sustained reductions in power demand across all flight phases.

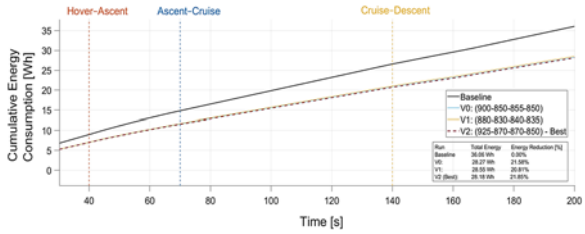

Fig. 8. Cumulative energy consumption for baseline and optimized rotor speed schedules over the mission.

The separation between the baseline and optimized trajectories increases progressively with time, with the largest divergence occurring during the cruise phase, where reduced rotor speed lowers power demand over an extended period. The optimized cases converge to similar energy profiles, indicating that different rotor speed schedules can achieve comparable levels of energy efficiency.

The best performing case (V2) achieves a total energy reduction from approximately 36.06 Wh to 28.18 Wh, corresponding to an energy reduction of about 21.85 %, confirming the effectiveness of rotor speed scheduling in reducing mission energy consumption.

The energy consumption distribution across individual flight phases is summarized in Fig. 9, which compares the energy required for each segment. Energy reductions are observed across all flight phases relative to the baseline. In hover, energy consumption decreases from approximately 9.0 Wh to 7.0 Wh, while in ascent it reduces from 5.9 Wh to 4.6 Wh. During cruise, the energy decreases from 11.7 Wh to 9.2 Wh, representing the largest absolute reduction due to the longer duration of this phase. A similar reduction is observed during descent, from 9.5 Wh to 7.4 Wh.

The results discussed in this section establish a clear relationship between rotor speed scheduling, reduced power demand, and improved energy efficiency. Lower rotor speeds reduce aerodynamic losses, particularly in forward flight, leading to sustained reductions in cumulative energy consumption across the mission.

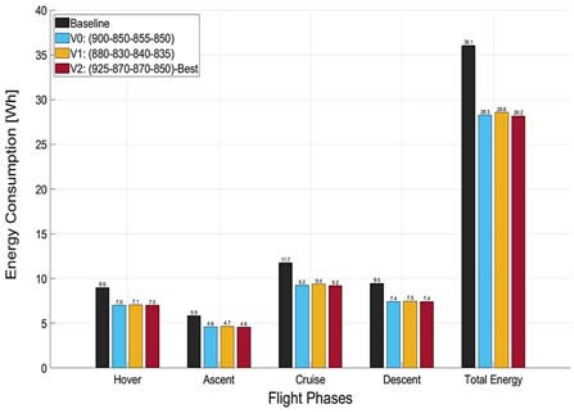

Fig. 9. Energy consumption across mission phases for the baseline and selected rotor speed schedules showing reduced total energy for the optimal case.

To provide a comprehensive overview of the evaluated rotor speed schedules, the results for all tested configurations are summarized in Table 3. A total of six candidate schedules were assessed in addition to the baseline case. The results show that all optimized configurations achieve significant reductions in total mission energy, with reductions exceeding 20 % across all cases.

4.3. Trajectory Optimization

In this section, trajectory optimization is performed within a sequential optimization framework using a fixed rotor speed schedule obtained from the preceding rotor speed optimization stage. The rotor speed profile (925, 870, 870, 850) is held constant for all optimized cases, allowing the influence of trajectory parameters on energy consumption to be isolated. Specifically, the ascent speed, cruise speed, descent speed, and cruise altitude are varied, while maintaining a consistent rotor operating condition across all simulations. By modifying these key parameters, the vehicle can

operate under more favorable aerodynamic conditions, thereby reducing overall energy demand.

The impact of trajectory design on mission energy consumption is evaluated by comparing the baseline case with two representative optimized trajectories, as illustrated in Figs. 10–13. The selected cases include the baseline profile (R0), the best performing optimized trajectory (R1), and a higher altitude alternative (R2), enabling assessment of both speed and altitude effects.

Table 3. Summary of rotor speed schedules and phase energy consumption across the mission.

Case	RPM Schedule	Total Energy (Wh)	Energy Reduction (%)	Phase Energy (Wh)			
				Hover	Ascent	Cruise	Descent
Baseline	(1000, 1000, 1000, 1000)	36.06	0.00	8.99	5.85	11.75	9.47
V0	(900, 850, 855, 850)	28.27	21.58	7.02	4.60	9.24	7.42
V1	(880, 830, 840, 835)	28.55	20.81	7.05	4.65	9.38	7.47
V2 (Best)	**(925, 870, 870, 850)**	**28.18**	**21.85**	**7.00**	**4.57**	**9.20**	**7.41**
V3	(925, 875, 870, 860)	28.20	21.78	7.00	4.57	9.21	7.43
V4	(900, 850, 845, 840)	28.37	21.33	7.02	4.60	9.30	7.44
V5	(860, 830, 855, 850)	28.49	20.97	7.09	4.66	9.32	7.42

The altitude profiles shown in Fig. 10 indicate that all trajectories follow similar mission structures with distinct phase transitions. The baseline and optimized case R1 maintain a cruise altitude of approximately 80 ft (24.4 m), while R2 operates at a higher cruise altitude of 90 ft (27.4 m). The climb and descent segments remain smooth across all cases, ensuring comparable mission feasibility. However, R1 exhibits a slightly earlier and more gradual descent initiation, which contributes to improved energy efficiency.

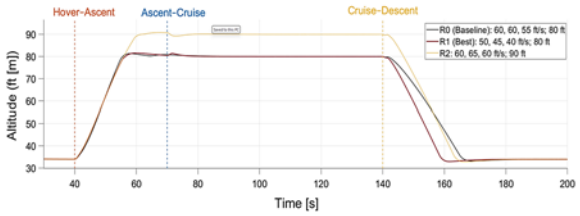

Fig. 10. Altitude profiles for baseline and optimized trajectory cases.

The corresponding airspeed profiles in Fig. 11 reveal the primary source of variation between trajectories. The baseline maintains a cruise speed of approximately 60 ft/s (18.3 m/s), whereas R1 adopts a reduced speed profile 50, 45, and 40 ft/s (15.2, 13.7, and 12.2 m/s), and R2 increases cruise speed to approximately 65 ft/s (19.8 m/s). These differences directly influence aerodynamic power requirements, particularly during the cruise phase where forward flight dominates energy consumption.

The effect of these trajectory modifications is clearly reflected in the main rotor power profiles presented in Fig. 12. The optimized trajectory R1 achieves a consistent reduction in power demand across all phases, with the most significant improvement observed during cruise. In this phase, the power requirement decreases substantially compared to the baseline, indicating that reduced forward speed effectively lowers profile and parasitic power components. In contrast, the higher altitude case R2 exhibits moderate power reduction relative to the baseline but remains less efficient than R1 due to increased aerodynamic loading associated with higher cruise speed.

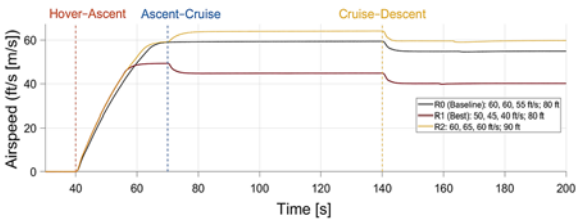

Fig. 11. Airspeed profiles showing variations in optimized trajectories.

The cumulative impact of these power reductions is shown in Fig. 13, where the total energy consumption over the mission is compared. The baseline case reaches approximately 36.06 Wh, while the optimized trajectory R1 reduces the total energy to 27.05 Wh, corresponding to an energy reduction of 24.99 %. The higher altitude case R2 achieves a smaller reduction of 19.74 %, confirming that altitude increase alone does not yield optimal performance without coordinated speed adjustment.

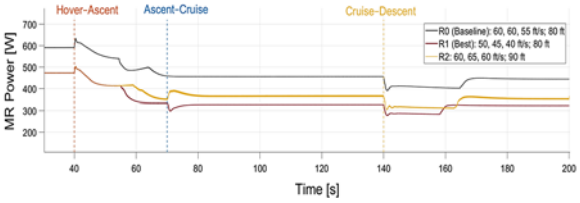

Fig. 12. Main rotor power comparison for baseline and optimized trajectories illustrating reduced power demand under optimized trajectory conditions.

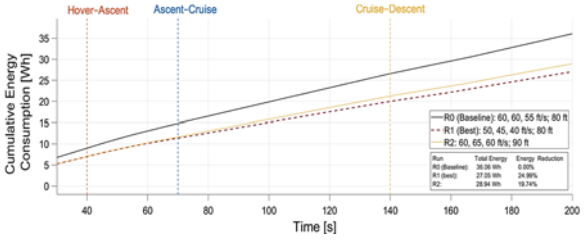

Fig. 13. Cumulative energy consumption showing 24.99 % reduction achieved through trajectory optimization.

These results demonstrate that trajectory optimization plays a critical role in reducing mission energy consumption. Specifically, reducing forward airspeed during energy intensive phases, particularly cruise, leads to substantial improvements in efficiency. While altitude variations influence performance, the results indicate that speed optimization is the dominant factor. The best performing trajectory (R1) achieves the lowest energy consumption by balancing reduced aerodynamic power demand with feasible flight dynamics, thereby establishing an effective strategy for mission-based energy optimization for electric UAV rotorcraft.

The results of the trajectory optimization study are summarized in Table 4. The variations in trajectory parameters lead to significant differences in total mission energy, despite identical rotor speed profiles. The baseline case, defined by a speed profile of 60, 60, and 55 ft/s (18.3, 18.3, and 16.8 m/s) and a cruise altitude of 80 ft (24.4 m), with a constant rotor speed of 1000 RPM, results in a total energy consumption of 36.06 Wh. In contrast, all optimized cases are evaluated using the prescribed rotor speed schedule, ensuring that only trajectory parameters are varied.

The optimized trajectories achieve substantial reductions, with energy reductions ranging from 19.74 % to 24.99 %. The best performing case, R1, reduces total energy to 27.05 Wh, corresponding to a 24.99 % improvement, primarily due to lower forward speeds during ascent, cruise, and descent. In contrast, higher speed or higher altitude configurations, such as R2 and R3, provide smaller benefits despite increased maximum true airspeed (TAS), indicating that higher aerodynamic loads offset potential efficiency gains. The reduced altitude case R4 also performs well, achieving a 23.06 % reduction, indicating that both speed and altitude influence energy consumption, though speed has a more dominant effect. Across all cases, maximum climb and descent rates remain within a narrow range, confirming that performance constraints are maintained. These results indicate that trajectory optimization, when performed under the fixed rotor speed schedule, provides substantial energy savings and represents a dominant contributor to overall mission efficiency within the proposed sequential optimization framework.

Table 4. Summary of trajectory optimization results obtained using a fixed rotor speed schedule derived from prior rotor speed optimization. The rotor speed profile is held constant for all optimized cases.

Case	Fixed Rotor Speed Schedule (RPM)	Trajectory Parameters (V_ascent, V_cruise, V_descent (ft/s [m/s]); h_cruise (ft [m]))	Total Energy (Wh)	Energy Reduction (%)	Max TAS (ft/s [m/s])	Max Climb (ft/s [m/s])	Max Descent (ft/s [m/s])
R0 (Baseline)	(1000, 1000, 1000, 1000)	(60, 60, 55 ft/s; 80 ft)	36.06	0.00	59.4	2.94	–1.85
R1 (Best)	**(925, 870, 870, 850)**	**(50, 45, 40 ft/s; 80 ft)**	**27.05**	**24.99**	**54.9**	**2.18**	**–1.88**
R2	(925, 870, 870, 850)	(60, 65, 60 ft/s; 90 ft)	28.94	19.74	64.1	2.18	–1.90
R3	(925, 870, 870, 850)	(60, 60, 55 ft/s; 90 ft)	28.18	21.85	59.4	2.18	–1.89
R4	(925, 870, 870, 850)	(60, 55, 50 ft/s; 70 ft)	27.74	23.06	59.0	2.18	–1.81
R5	(925, 870, 870, 850)	(60, 60, 60 ft/s; 80 ft)	28.52	20.89	59.7	2.18	–1.94

4.4. Joint Optimization Analysis

This section evaluates the simultaneous optimization of rotor speed scheduling and flight trajectory to assess their combined impact on mission energy consumption. While the previous sections examined these strategies independently, their interaction can produce additional performance gains that are not achievable through isolated optimization. By jointly adjusting rotor speed and trajectory parameters, the system can better balance aerodynamic and rotor power requirements across all flight phases. The following analysis compares the joint approach with the baseline and individually optimized cases, with emphasis on total energy consumption, power distribution, and operational efficiency.

A parametric search was conducted by integrating optimized trajectory parameters with varying rotor speed schedules, as summarized in Table 5. The baseline case employs a constant rotor speed, whereas the combined cases (C1–C6) implement reduced rotor speeds alongside optimized flight path parameters. All combined configurations demonstrate significant reductions in total energy compared to the baseline.

Among the evaluated cases, C1 achieves the lowest total energy consumption of 27.04 Wh, corresponding to a 25.01 % reduction relative to the baseline. Notably, cases C2, C3 and C4 yield nearly identical energy values despite slight variations in rotor speed schedules, indicating the presence of a relatively flat optimum region. This behavior suggests that the combined solution is robust to moderate changes in rotor speed when the trajectory parameters are maintained.

Table 5. Joint optimization results for rotor speed and trajectory parameters.

Case	RPM Schedule	Trajectory Parameters (V_ascent, V_cruise, V_descent (ft/s [m/s]); h_cruise (ft [m]))	Total Energy (Wh)	Energy Reduction (%)
Baseline	(1000, 1000, 1000, 1000)	(60, 60, 55 ft/s; 80 ft)	36.06	0.00
C1 (Best)	**(935, 880, 870, 850)**	**(50, 45, 40 ft/s; 80 ft)**	**27.04**	**25.01**
C2	(925, 870, 870, 850)	(50, 45, 40 ft/s; 80 ft)	27.05	24.99
C3	(915, 860, 860, 845)	(50, 45, 40 ft/s; 80 ft)	27.05	24.97
C4	(935, 880, 880, 855)	(50, 45, 40 ft/s; 80 ft)	27.05	24.99
C5	(925, 870, 870, 850)	(50, 50, 40 ft/s; 80 ft)	27.20	24.57
C6	(925, 870, 870, 850)	(50, 45, 45 ft/s; 80 ft)	27.15	24.70

In contrast, Cases C5 and C6 introduce small deviations from the optimal trajectory by modifying the cruise and descent speeds, respectively. In C5, the cruise speed is increased from 45 ft/s (13.7 m/s) to 50 ft/s (15.2 m/s), leading to higher aerodynamic power during forward flight and a corresponding increase in energy consumption. In C6, the descent speed is increased from 40 ft/s (12.2 m/s) to 45 ft/s (13.7 m/s), reducing the efficiency of the low power descent phase. These deviations result in slightly higher total energy values compared to the best case, highlighting the sensitivity of the solution to forward speed selection, particularly during cruise.

The underlying control mechanism of the combined solution is illustrated in Fig. 14 which compares the baseline constant rotor speed with the optimized schedule. The baseline maintains a fixed value of 1000 RPM throughout the mission, whereas the optimized schedule adapts to the trajectory. Reduced rotor speeds are maintained during cruise and descent, where aerodynamic loading is lower, while slightly higher values are preserved during hover and ascent to satisfy thrust requirements. This variation reflects the changing balance between induced and profile power, where lower rotor speeds are advantageous in forward flight conditions. The smooth transitions between phases also indicate that the optimized schedule remains physically realizable and avoids abrupt control inputs.

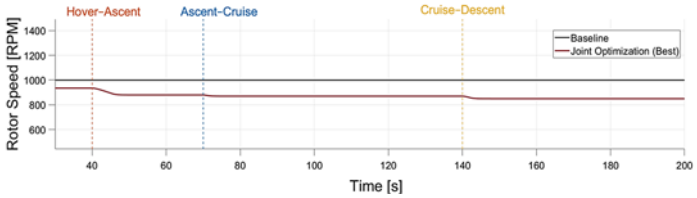

Fig. 14. Rotor speed schedule for baseline and joint optimization across flight phases.

The impact of this optimized control strategy on power demand is shown in Fig. 15. The combined case reduces power demand across all flight phases, with the most pronounced reductions occurring during cruise and transition periods. In these phases, the simultaneous reduction of rotor speed and forward airspeed lowers both profile and parasitic power components, leading to a more efficient operating condition. Compared to the individual optimization cases, the joint strategy achieves a more uniform reduction in power, indicating improved overall system efficiency.

The improvement achieved through the joint optimization is illustrated in Fig. 16, where cumulative energy consumption is compared across the baseline, individual optimization cases, and the joint approach. The joint optimization consistently exhibits the lowest energy accumulation throughout the mission, indicating that the benefits of rotor speed reduction and trajectory shaping are complementary rather than redundant.

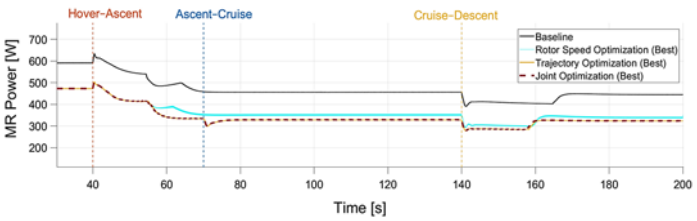

Fig. 15. Main rotor power comparison for baseline, rotor speed optimization, trajectory optimization, and joint optimization.

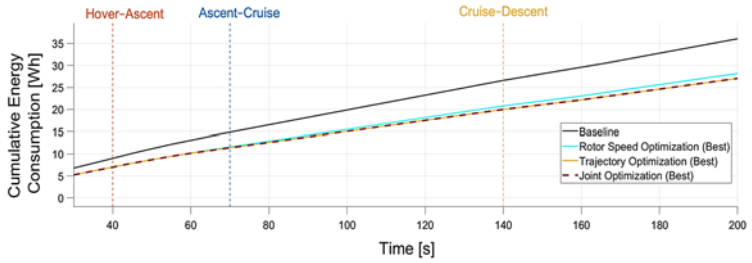

Fig. 16. Cumulative energy consumption for baseline, rotor speed optimization, trajectory optimization, and joint optimization.

The quantitative comparison of the different optimization strategies is summarized in Table 6. The baseline case requires a total energy of 36.06 Wh. Rotor speed optimization reduces this to 28.18 Wh, corresponding to a 21.85 % reduction. Trajectory optimization provides a greater improvement, lowering total energy to 27.05 Wh (24.99 %), which represents an additional 4.01 % improvement relative to rotor speed optimization.

Table 6. Total mission energy consumption and relative performance comparison of rotor speed optimization, trajectory optimization, and joint optimization.

Case	Total Energy (Wh)	Energy Saving (%)	Improvement vs Rotor Speed Optimization (%)	Improvement vs Trajectory Optimization (%)
Baseline	36.006	0.00	-	-
Rotor speed optimization	28.18	21.85	0.00	-4.18
Trajectory Optimization	27.05	24.99	4.01	0.00
Joint Optimization	27.04	25.01	4.05	0.04

The joint optimization achieves the lowest total energy consumption of 27.04 Wh, corresponding to a 25.01 % reduction from the baseline. This represents a 4.05 % improvement relative to rotor speed optimization and a marginal additional improvement of 0.04 % over trajectory optimization. Given the small magnitude of this difference, the additional gain may fall within numerical tolerance or model uncertainty and should be interpreted with caution.

These results indicate that trajectory optimization provides the dominant contribution to energy reduction, while rotor speed scheduling offers incremental benefits when combined with trajectory optimization. However, further analysis, such as convergence or sensitivity studies, influence of environmental and operational uncertainties would be required to establish the robustness of this additional gain. The improvements are primarily driven by reduced power demand during cruise, with additional contributions from optimized ascent and descent profiles.

All simulations are performed under standard atmospheric conditions without explicitly considering wind, turbulence, or parameter uncertainty. These assumptions were intentionally adopted to provide a controlled environment for isolating the effects of rotor speed scheduling and trajectory optimization on mission energy consumption.

Variations in environmental conditions, vehicle mass, and battery state are expected to influence the absolute energy values reported. In particular, increased mass would primarily affect induced power during hover and ascent, while wind conditions would alter optimal trajectory parameters, especially during cruise. However, the core findings of this study are based on the interaction between rotor speed and aerodynamic loading, which governs the relative trends observed across optimization strategies. These underlying physical relationships are expected to remain consistent under moderate variations in operating conditions.

Therefore, while absolute energy savings may vary, the relative performance and benefits of the joint optimization framework are expected to remain qualitatively robust. Future work will extend the present analysis by incorporating environmental disturbances, parameter uncertainty, and adaptive mission planning under more realistic operating conditions.

5. Conclusions

This study presented an integrated framework for minimizing mission energy consumption in an electric rotorcraft through rotor speed scheduling and trajectory optimization. A physics-based simulation

model was used to evaluate the influence of rotor speed and trajectory parameters on power demand and cumulative energy consumption over a complete mission profile.

The results show that trajectory optimization provides the dominant contribution to energy reduction, while rotor speed scheduling offers complementary improvements within the sequential optimization framework. The rotor speed scheduling achieves a reduction of 21.85 %, while trajectory optimization yields a larger reduction of 24.99 % relative to the baseline. When both strategies are applied simultaneously, the combined optimization achieves the lowest total energy consumption of 27.04 Wh, corresponding to an overall reduction of 25.01 %.

Analysis of rotor speed, main rotor power, and cumulative energy profiles shows that the primary mechanism for energy reduction is the decrease in power demand during cruise, where reduced forward speed and lower rotor speed minimize aerodynamic losses. The joint optimization further improves efficiency by coordinating rotor speed with trajectory changes, resulting in consistent power reductions across all flight phases.

Although the additional improvement of combined optimization over trajectory optimization alone is modest, approximately 0.04 %, this difference may fall within numerical tolerance or model uncertainty and should therefore be interpreted with caution. The results nevertheless indicate consistent behavior between rotor speed scheduling and trajectory optimization, suggesting that the joint approach operates within a region close to the minimum achievable energy, with diminishing returns beyond trajectory optimization. The observed behavior also indicates a relatively flat optimum region, implying that comparable energy performance can be achieved under moderate variations in control parameters.

Overall, the findings highlight the importance of jointly considering trajectory and rotor speed in the design of energy-efficient rotorcraft operations. The proposed approach provides a systematic methodology for evaluating mission-based energy performance and can be extended to more complex scenarios, including variable environmental conditions, additional constraints, and real-time optimization strategies.

Acknowledgements

The authors express their gratitude for the computational facilities and simulation tools that made this research possible.

References

[1]. E. Chijioke, M. Żugaj, Comparative and joint optimization of rotor speed and trajectory for energy efficient electric Unmanned Aerial Vehicle (UAV) helicopters, in *Proceedings of the 2nd International Conference on Drones and Unmanned Systems (DAUS'26)*, 2026, pp. 191-197.

[2]. M. Shamiyeh, J. Bijewitz, M. Hornung, A review of recent personal air vehicle concepts, in *Proceedings of the Aerospace Europe 6th CEAS Conference*, 2017, pp. 1-18.

[3]. M. D. Moore, B. Fredericks, Misconceptions of electric propulsion aircraft and their emergent aviation markets, in *Proceedings of the 52nd Aerospace Sciences Meeting*, 2014, 0535.

[4]. B. J. Brelje, J. R. R. A. Martins, Electric, hybrid, and turboelectric fixed-wing aircraft: A review of concepts, models, and design approaches, *Progress in Aerospace Sciences*, Vol. 104, 2019, pp. 1-19.

[5]. J. G. Leishman, Principles of Helicopter Aerodynamics (2nd Ed.), *Cambridge University Press*, New York, 2006.

[6]. W. Johnson, Rotorcraft Aeromechanics, *Cambridge University Press*, New York, 2013.

[7]. W. Garre, T. Pflumm, M. Hajek, Enhanced efficiency and flight envelope by variable main rotor speed for different helicopter configurations, in *Proceedings of the 42nd European Rotorcraft Forum*, 2016, pp. 722-735.

[8]. M. Mistry, F. Gandhi, Helicopter performance improvement with variable rotor radius and RPM, *Journal of the American Helicopter Society*, Vol. 59, Issue 4, 2014, 042010.

[9]. D. Han, V. Pastrikakis, G. N. Barakos, Helicopter performance improvement by variable rotor speed and variable blade twist, *Aerospace Science and Technology*, Vol. 54, 2016, pp. 164-173.

[10]. H. Rienecker, V. Hildebrand, H. Pfifer, Energy optimal 3D flight path planning for unmanned aerial vehicle in urban environments, *CEAS Aeronautical Journal*, Vol. 14, 2023, pp. 621-636.

[11]. L. Deori, S. Garatti, M. Prandini, A model predictive control approach to aircraft motion control, in *Proceedings of the American Control Conference (ACC'15)*, 2015, pp. 2299-2304.

[12]. G. Su, X. Cheng, X. Liu, J. Jiang, Flight path optimization with optimal control method, *arXiv*, 2024, arXiv:2405.08306.

[13]. E. C. Suicmez, A. T. Kutay, Optimal path tracking control of a quadrotor UAV, in *Proceedings of the International Conference on Unmanned Aircraft Systems (ICUAS'14)*, 2014, pp. 115-125.

[14]. D. C. Gandolfo, L. R. Salinas, A. S. Brandão, J. M. Toibero, Path following for unmanned helicopter: An approach on energy autonomy improvement, *Information Technology and Control*, Vol. 45, Issue 1, 2016, pp. 86-98.

[15]. A. M. Mendoza, R. M. Botez, Commercial aircraft trajectory optimization to reduce flight costs and pollution: Metaheuristic algorithms, in Advances in Visualization and Optimization Techniques for Multidisciplinary Research (D. Vucinic, F. R. Leta, S. Janardhanan, Eds.), *Springer*, Singapore, 2020, pp. 33-62.

[16]. H. Kasmi, S. Laporte, R. M. Botez, Holistic approach for aircraft trajectory optimization using optimal control, *Journal of Aircraft*, Vol. 60, Issue 4, 2023, pp. 1302-1313.

[17]. A. Visintini, T. D. P. Perera, A. V. Savkin, A. Zanella, 3-D trajectory optimization for fixed-wing UAV-enabled wireless network, IEEE Access, Vol. 9, 2021, pp. 35045-35056.

[18]. M. A. Sadi, A. Jamali, N. M. N. Al-Falahi, M. F. Hossain, et al., Cascade model predictive control for enhancing UAV quadcopter stability and energy efficiency in wind turbulent mangrove forest environment, *e-Prime – Advances in Electrical Engineering, Electronics and Energy*, Vol. 10, 2024, 100836.

[19]. I. Nagy, E. Laufer, Energy-optimized 3D path planning for unmanned aerial vehicles, *Applied Sciences*, Vol. 14, Issue 16, 2024, 6988.

[20]. F. Yacef, N. Rizoug, L. Dala, C. Machado, Energy-efficiency path planning for quadrotor UAV under wind conditions, in *Proceedings of the 7th International Conference on Control, Decision and Information Technologies (CoDIT'20)*, 2020, pp. 1133-1138.

[21]. M. Żugaj, M. Edawdi, G. Iwański, S. Topczewski, et al., An unmanned helicopter energy consumption analysis, *Energies*, Vol. 16, Issue 4, 2023, 2067.

Published by International Frequency Sensor Association (IFSA) Publishing, S. L., 2026 (https://www.sensorsportal.com).